

Adsorption and Desorption Dynamics of Linear Polymer Chains to Spherical Nanoparticles: A Monte Carlo Investigation

Peter J. Dionne,[†] Catalin R. Picu,^{*,†} and Rahmi Ozisik^{*,‡}

Department of Mechanical, Aerospace and Nuclear Engineering and Department of Materials Science and Engineering, Rensselaer Polytechnic Institute, Troy, New York 12180

Received December 29, 2005; Revised Manuscript Received February 21, 2006

ABSTRACT: Dynamics of attachment/detachment processes of chains to/from spherical fillers in a polymer nanocomposite is investigated by means of numerical simulations using a chemistry-specific model for the polymer. The effects of polymer–particle interaction, chain length, chain-to-filler distance, and filler radius on the attachment/detachment processes are studied. It is found that the time a chain is in contact with a filler scales with the number of attached beads following a power law. Increasing the energetic interaction parameter between polymer and filler slows the detachment process, and the system average characteristic detachment time follows an Arrhenius law in which the activation energy is proportional to the polymer–particle energetic interaction parameter.

Introduction

Polymer nanocomposites are unique materials because of the large observed change in material properties associated with the addition of a small volume fraction of nanometer-sized filler particles.^{1–6} For example, when a small volume fraction of spherical nanoparticles are added to a polymer, the viscosity increases up to an order of magnitude compared to the neat polymer,² low strain amplitude shear storage modulus increases over an order of magnitude,⁴ and the low-frequency storage and loss modulus increases several orders of magnitude.³

These property changes are observed when the size of the filler is comparable to that of the polymer chains and to the average wall-to-wall distance between fillers. Under such conditions, and with good dispersion of fillers within the matrix, it is believed that a secondary network of polymer chains connecting filler particles forms.^{2–5} This transient network is believed to be the cause of the large enhancement observed in viscoelastic properties. The transient network also produces a rubberlike behavior in a certain range of frequencies.³ The appearance and range of this regime depend on the polymer–filler affinity and, hence, on the lifetime of attachments between fillers and bridging chains.

This study involves the investigation of the dependence of residence time on various system parameters. This information is crucial in modeling the dynamic behavior of nanocomposites on larger scales. The present analysis is part of a broader program concerned with the development of molecular rheological models for polymers filled with nanoparticles.^{7,8}

Simulation Setup

The simulation method uses a Monte Carlo (MC) technique first proposed by Mattice and colleagues. Polyethylene (PE) chains are represented by a coarse-grained rotational isomeric state (RIS) model.⁹ The coarse-grained model was obtained by combining every two carbon and associated hydrogen atoms on the PE chain into a bead that is located on a high coordination lattice (named second-nearest-neighbor diamond lattice, SNND).

The short-range intramolecular potential energy of the PE chains was calculated using the coarse-grained RIS model, and the long-range intramolecular and intermolecular interaction potential energies were calculated using a lattice-based approximation of the Lennard-Jones potential.

The polymer beads were constrained to single bead moves that were random, physically realistic, and resulted in only local conformation changes. The moves were accepted on the basis of the Metropolis algorithm. This results in the system mimicking the random thermal motions of molecules in a real polymer system. This allows us to make a relative comparison of the dynamic properties between chains in bulk and those near filler surfaces. The applicability of this simulation method to the study of dynamic properties of polyethylene has been shown for polyethylene melts^{10,11} and thin films.^{12,13} Details of the simulation method and the potentials employed for PE can be found in refs 14 and 15.

The simulations were performed for a temperature of 200 °C, representing a melt. The system remained amorphous with densities of ~ 0.76 g/cm³. The base simulation cell of the SNND lattice is a parallelepiped where the angle between each pair of the three intersecting edges is 60°. A single filler particle was located in the center of the base simulation cell, and periodic boundary conditions were applied in all directions, resulting in the filler particles forming a close-packed sphere structure. This creates systems that represent bulk material with spherical nanometer-sized particles homogeneously dispersed. The particle radius and the distance between particles were both comparable to the radius of gyration of PE chains in the neat melt. The filler particle was kept stationary during the simulation. The size of the simulation cell was larger than twice the chain radius of gyration R_g to prevent chains from interacting with themselves through the periodic boundary conditions and to minimize the overall size of the system.

The energetic interaction, $u(r)$, between polymer beads and particle beads was defined using the same Lennard-Jones potential used for the polymer-to-polymer interactions, except it was scaled by a prefactor, w . This parameter represents the polymer–filler affinity and was varied from $w = 0.1$ to $w = 8.0$, such that both slightly repulsive and strongly attractive interactions were considered in separate simulations. The polymer–filler interaction is modeled generically and can

[†] Department of Mechanical, Aerospace and Nuclear Engineering.

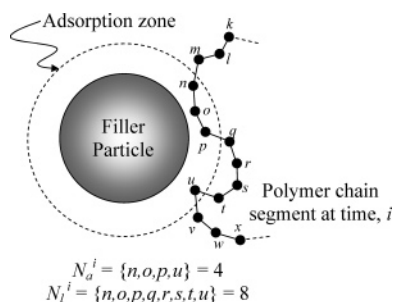
[‡] Department of Materials Science and Engineering.

* Corresponding authors: C. Picu (picu@rpi.edu) or R. Ozisik (ozisik@rpi.edu).

Table 1. Details of the Systems Investigated^a

system identifier	L	L/R_g	N	N_c	N_f	D_f/R_g	D/R_g	φ (%)	w	$\tau_R/\tau_R^{\text{neat}}$ ($p = 1$)	$\langle N_a \rangle$	$\tau_{\text{ad}}/\tau_R^{\text{neat}}$
S1	$19 \times 18 \times 18$	2.53	80	14	0					1.0	13.2 ^b	
S3	$18 \times 18 \times 18$	2.53	80	13	1	0.70	1.83	1.59	0.1	1.04	11.0	0.0410
S4	$18 \times 18 \times 18$	2.53	80	13	1	0.70	1.83	1.59	1	0.98	13.4	0.0956
S5	$18 \times 18 \times 18$	2.53	80	13	1	0.70	1.83	1.59	2	1.25	15.4	0.198
S14	$21 \times 22 \times 22$	6.37	6	126	0					1.0		
S15	$21 \times 20 \times 20$	2.75	220	7	0					1.0		
S16	$15 \times 15 \times 15$	3.09	40	15	0					1.0		
S17	$18 \times 18 \times 18$	2.53	80	13	1	0.70	1.83	1.59	4	1.31	21.1	1.03
S18	$18 \times 18 \times 18$	2.53	80	13	1	0.70	1.83	1.59	6	1.65	27.3	3.39
S19	$18 \times 18 \times 18$	2.53	80	13	1	0.70	1.83	1.59	8	1.54	31.1	7.93

^a L = simulation cell size, N = chain length, N_c = number of chains, N_f = number of particles, D_f = particle diameter, D = wall-to-wall distance, φ = volume fraction of filler (%), w = monomer–particle interaction parameter, τ_R = Rouse time, $\langle N_a \rangle$ = average number of adsorbed beads per chain, and τ_{ad} = characteristic time. ^b The average number of adsorbed beads per chain is calculated for a virtual filler with $D_f/R_g = 0.7$. See text for explanation.

Figure 1. Definition of the measures of chain adsorption, N_a^i and N_l^i .

represent the range of interactions including both physical and chemical adsorption; however, the range over which w is varied in this study most likely represents physical adsorption. The details of the various systems investigated are presented in Table 1.

Two sets of simulations were performed. The first set had a fine temporal resolution and spanned approximately one Rouse relaxation time for each system. The second set used a coarse temporal resolution and spanned approximately ten Rouse relaxation times. The fine resolution data were used to determine the residence time of the chains, while the coarse resolution simulations were used to determine the ensemble average of polymer beads adsorbed on the filler surface. All simulations were equilibrated for at least five times the Rouse relaxation time of the polymer chains.

Results and Discussion

The number of adsorbed beads per chain N_a^i and the length of the chain segment interacting with the filler particle N_l^i at an instant in time, i , were two measures of the magnitude of chain adsorption considered. An example of the two measures N_a^i and N_l^i is shown in Figure 1. The value of N_a^i is determined by counting the number of polymer beads per chain located within an adsorption zone around the filler particle at time i . These beads are said to be in contact with the filler. The adsorption zone is defined by the range of the polymer–filler potential and contains three lattice sites in the radial direction. The value of N_l^i is the number of chain beads between (and including) the first and the last bead in contact with the filler particle on a chain. Note that $N_l^i \geq N_a^i$, as the adsorbed chain segment N_l^i may include loops.¹⁵

The two measures N_a^i and N_l^i exhibit a high-frequency oscillation overlapped on lower frequency components. A chain may come in contact with the filler, build up contacts, and then diffuse away from the filler. This lower frequency process is of interest here. An adsorption/desorption event is defined as a span of the simulation in which N_a^i is continuously greater

than zero. The duration of the adsorption/desorption event is equal to the residence time of that chain, t_{ad} . From these data, it is possible to estimate the averages of the two fluctuating functions over each t_{ad}

$$\overline{N_k} = \overline{N_k(t_{\text{ad}})} = \frac{1}{n_{\text{ad}}} \sum_{j=1}^{n_{\text{ad}}} \frac{1}{t_{\text{ad}}} \sum_{i=1}^{t_{\text{ad}}} N_k^i \quad (1)$$

where the subscript k is either “a” or “l” and n_{ad} is the number of adsorption/desorption events whose duration is equal to t_{ad} . Another measure considered is N_a^{max} , the maximum value of N_a^i during an adsorption/desorption event of length t_{ad} . The average value of N_a^{max} , $\overline{N_a^{\text{max}}}$, also a function of t_{ad} , is performed over all n_{ad} and is shown in eq 2.

$$\overline{N_a^{\text{max}}} = \overline{N_a^{\text{max}}}(t_{\text{ad}}) = \frac{1}{n_{\text{ad}}} \sum_{j=1}^{n_{\text{ad}}} N_a^{\text{max}} \quad (2)$$

The relationship between $\overline{N_a}$, $\overline{N_l}$ and t_{ad} is shown in Figure 2. The adsorption time is normalized here by the Rouse relaxation time in the neat polymer, τ_R^{neat} . The two functions are described over a broad range of t_{ad} by power laws with power indices of 0.50 and 0.25 for $\overline{N_l}$ and $\overline{N_a}$, respectively. Also, it is observed that the curves shift downward as the polymer–particle interaction parameter, w , increases (see inset to Figure 2b). At long residence times, a transition to a plateau is observed. The plateau is more obvious in Figure 2b and becomes even more apparent when smaller chain lengths are considered, as discussed below.

It also must be noted that the curve for the neat system (S1) has the same shape and slope as the systems containing filler particles, the only difference being a vertical shift of the (S1) curves relative to the other systems. The data for the neat system were collected considering a virtual “filler” of same size as that used in the model of the composite. The chain was considered to be “attached” as long as at least one of its beads was present in an annular zone around the virtual filler, where the zone size is identical to that used to define attachment in the filled systems (Figure 1). The similitude between (S1) and the filled systems shown in Figure 2 indicates that the general shape of the function is controlled by the geometry of the problem. This observation is further supported by previous findings^{15,16} that the Gaussian statistics of the chain conformations is not affected by the excluded volume of the filler.

There appears to be a contradiction in Figure 2 in that the curve for the neat system (S1) is shifted the most compared to the filled systems (S4, S5, S17, and S18). However, it must be noted that it is not proper to quantitatively compare the vertical

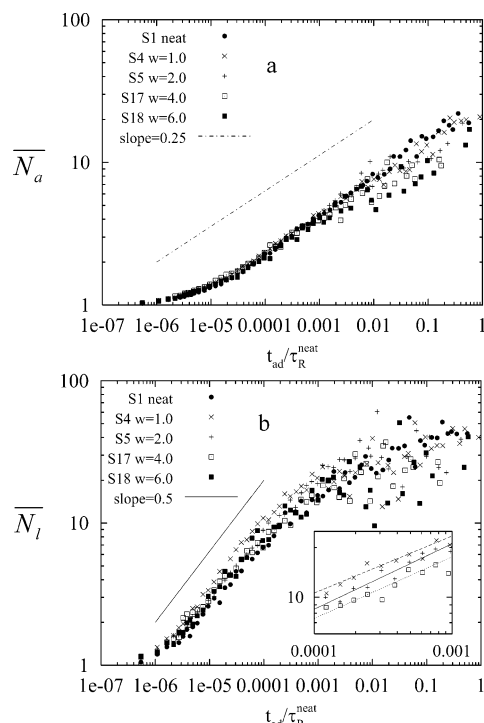


Figure 2. (a) Average number of adsorbed beads per chain vs chain residence time. (b) Average length of adsorbed segment vs chain residence time for $w = 1, 2, 4$, and 6 . The inset to (b) shows a detail of the curves in the main figure evidencing the shifting of curves in the vertical direction as the adsorption parameter w increases.

shift of the (S1) curve to the curves for the filled systems because of an inconsistency in what is being measured between the neat and filled systems.

The attachment–detachment process involves two distinct physical phenomena: the random walk of the chain in the close neighborhood of the filler, which is well described by the Rouse model,¹⁷ and its diffusion to/from the filler on longer time and spatial scales.¹⁸ The linear portion of the curves in Figure 2b is due to the Rouse motion of the adsorbed chain segments. To illustrate the Rouse scaling, consider the Rouse time for mode p , where ζ is the friction coefficient, b is the Kuhn segment length, k_b is the Boltzmann's constant, and N is the number of Kuhn segments per chain:

$$\tau_p = \frac{\zeta b^2}{3\pi^2 k_b T} \left(\frac{N}{p} \right)^2 \quad (3)$$

Identifying $N/p = \bar{N}_l$ and $\tau_p = t_{ad}$, one may write

$$\log(\bar{N}_l) = \frac{1}{2} \log(t_{ad}) - \frac{1}{2} \log\left(\frac{\zeta b^2}{3\pi^2 k_b T}\right) \quad (4)$$

This justifies the 0.5 slope of the curve in Figure 2b at small and moderate t_{ad} . To further confirm this interpretation, eq 3 was used to infer N/p corresponding to a Rouse time equal to t_{ad} and using ζ determined previously for the same filled system.¹⁵ This quantity was then plotted versus \bar{N}_l , and a linear relationship was obtained.

The vertical shift of the curves in Figure 2b with increasing w is due to the increase of the local, apparent friction of the chains induced by the energetic interaction with fillers. This shift is captured by the second term on the right-hand side of eq 4. The variation of the friction coefficient ζ with the polymer–filler affinity w was studied in ref 15.

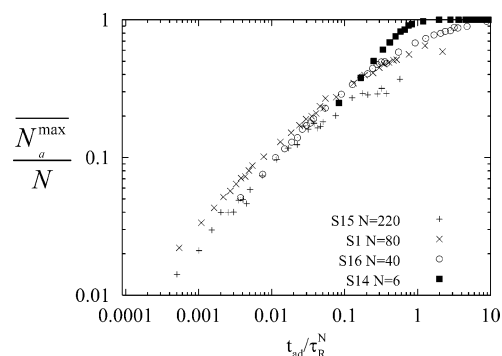


Figure 3. Average maximum number of adsorbed beads per chain vs chain residence time for chains of various lengths.

The relationship between \bar{N}_a and \bar{N}_l represented in Figure 2a,b depicts the number of beads effectively attached and the length of a chain segment engaged in the interaction with the filler. The data suggest a relationship of the form $\bar{N}_a \sim \bar{N}_l^{1/2}$, which is in agreement with the classical scaling argument for flat surfaces (cf. ref 19). Additionally, it is noted that linear scaling was used in other works.⁹

It is interesting to investigate the nature of the plateau to which all curves appear to asymptote at large t_{ad} (Figure 2b).

The plateau appears better defined when looking at \bar{N}_a^{\max} and in systems with smaller chain lengths. To avoid inconsistencies associated with changing the filler size (note that the filler and chain size must be comparable) and in view of the similitude between the curve for the neat system (S1) and the curves for the filled systems (Figure 2), this issue is studied by using various neat systems. Neat systems with N ranging from 6 to 220 are used for this purpose. The results are shown in Figure 3.

The plateau is related to the relative magnitude of the chain, filler, and adsorption volume size. If we consider a chain much smaller than the size of the filler, the plateau value of \bar{N}_a^{\max} will be the chain length N (i.e., there is a nonzero probability that the whole chain is adsorbed). At the other extreme, a chain that is much larger than the size of the filler should have a plateau value of \bar{N}_a^{\max} that approaches the maximum bead capacity of the adsorption zone, a value smaller than N . This can be seen in the \bar{N}_a^{\max} vs t_{ad} plot in Figure 3, where \bar{N}_a^{\max} is normalized by the chain length and t_{ad} by the Rouse time of the respective neat chain system. In our systems, where the chain radius of gyration and the filler radius are similar, the probability to find fully adsorbed chains does not vanish, and the plateau value approaches $\bar{N}_a^{\max}/N = 1$.

The start of the transition from slope 0.5 (Figure 2b) to the plateau is conjectured to be purely geometric in nature and not related to excluded-volume interactions with the filler. This is supported by the observation that the transition has similar width, regardless of whether the filled or the neat systems are considered. The possibility that the departure from the Rouse prediction (slope 0.5) is related to entanglement effects also was investigated. In the simulations described here the chains cannot cross, and hence, effects due to chain entanglement should be seen. To eliminate the effects of entanglements, a system of phantom chains ($N = 220$) was examined. The transition is observed in this system as well, which eliminates the possibility that entanglements play a role. Another supporting observation is the slope of the curves in Figure 3, for chain lengths ranging from unentangled ($N = 6$) to moderately entangled ($N = 220$), is insensitive to N .

The possibility that the transition is a result of highly adsorbed chains possessing different conformations, and therefore different adsorption dynamics than the average chain, was investigated next. Chains that stay adsorbed for very long times were selected, and the statistics of their end-to-end vectors were computed. It was concluded that their conformations are not different than other chains in the same system (and in the bulk, for that matter). This conclusion is similar to previous studies which showed the statistics of chain conformations is not affected by topological interactions with the filler (excluded volume).^{15,16}

The dynamics of the adsorption/desorption process described by the data in Figure 2 is not sensitive to the position of the center of mass of the respective chain relative to the surface of the filler. The issue was investigated by assigning the chains into shells (bins) around the filler based on the distance from their center of mass to the filler surface. The distance between the center of mass of the polymer and the filler surface was varied from zero to half of the wall-to-wall distance between neighboring fillers. A plot similar to Figure 2 was drawn for each bin, and no difference was observed between these plots within the accuracy of these simulations.

Apart from the details of the attachment–detachment process discussed above, an estimate of the overall average attachment time for a given system, t_{ad} , is desirable as it may be used in mesoscopic rheological modeling of the nanocomposites.⁸ The obvious procedure for finding this quantity would be to find the mean of the probability distribution function (PDF) of t_{ad} determined from the simulation. However, as mentioned above, this distribution is dominated by very short lifetimes. Recent investigations similarly found that the dynamics of desorbing chains can be grouped into rapid and slow events.¹⁸ Clearly, viscoelasticity is controlled by the slow events; hence, in computing the average, it is desirable to filter out the high-frequency fluctuations.

A simple procedure to filter out high-frequency fluctuations is to compute the average attachment time as $\tau_{ad} = t_{ad}(w, N_a = \langle N_a \rangle)$, where the function $t_{ad}(w, N_a)$ is determined for each respective system using the data shown in Figure 2a and $\langle N_a \rangle$ is the ensemble average of the number of beads adsorbed per chain. The resulting values of τ_{ad} for the various systems are shown in Table 1.

Next, the relationship between the system average attachment lifetime and the polymer–filler affinity parameter, w , can be determined. The variation of t_{ad} with w is shown in Figure 4 in a semilog plot. An Arrhenius dependence of the form

$$\tau_{ad}(w) = c_1 e^{c_2 w} \quad (5)$$

is suggested by the data, where c_1 and c_2 are constants. The slight deviation of the data points for $w = 6.0$ and $w = 8.0$ is most likely a result of insufficient statistics. Interestingly, the information about the geometry and the chain size is contained in the preexponential constant c_1 . The constant c_2 is inversely

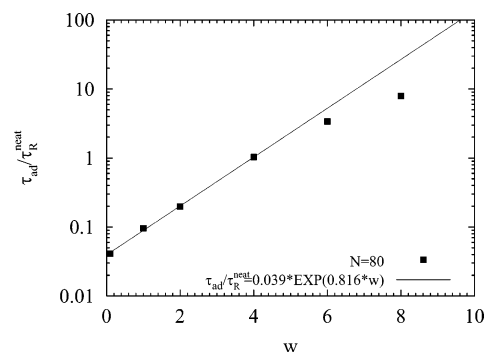


Figure 4. Characteristic attachment/detachment time as a function of the polymer–particle energetic interaction parameter, w .

proportional to the temperature, as observed from simulations at various temperatures. When this relation is used in molecular models aimed at capturing the rheology of the composite, the two constants must be determined for the respective system from this type of chemically specific simulations (see legend in Figure 4).

Conclusions

The dynamics of the adsorption/desorption process of chains from spherical fillers in a polymer nanocomposite was investigated by means of Monte Carlo simulations. It was observed that attachment time scales with the number of attached beads following a power law. The physical explanation for this behavior resides in the Rouse motion of the chains. This scaling holds for many decades in time. The system average attachment time follows an Arrhenius dependence on the magnitude of the energetic interaction between polymers and filler. This study is relevant for the construction of molecularly informed models of the rheology of polymer nanocomposites.

References and Notes

- (1) Wei, L.; Tang, T.; Huang, B. *J. Polym. Sci., Part A* **2004**, *42*, 941.
- (2) Zhang, Q.; Archer, L. *Macromolecules* **2004**, *37*, 1928.
- (3) Zhang, Q.; Archer, L. *Langmuir* **2002**, *18*, 10435.
- (4) Steinstein, S. S.; Zhu, A. *Macromolecules* **2002**, *35*, 7262.
- (5) Zhu, Z.; Thompson, T.; Wang, S. Q.; von Meerwall, E. D.; Halasa, A. *Macromolecules* **2005**, *38*, 8816.
- (6) Ozisik, R.; Zheng, J.; Dionne, P. J.; Picu, C. R.; von Meerwall, E. D. *J. Chem. Phys.* **2005**, *123*, 134901.
- (7) Sarvestani, A.; Picu, R. C. *Polymer* **2004**, *45*, 7779.
- (8) Sarvestani, A.; Picu, R. C. *Rheol. Acta*, in press.
- (9) Wang, Y.; Rajagopalan, R.; Mattice, W. L. *Phys. Rev. Lett.* **1995**, *74*, 2503.
- (10) Doruker, P.; Mattice, W. L. *Macromol. Symp.* **1998**, *133*, 47.
- (11) Ozisik, R.; Doruker, P.; Mattice, W. L.; von Meerwall, E. D. *Comput. Theor. Polym. Sci.* **2000**, *10*, 411.
- (12) Doruker, P.; Mattice, W. L. *Macromolecules* **1999**, *32*, 194.
- (13) Doruker, P.; Mattice, W. L. *J. Phys. Chem. B* **1999**, *103*, 178.
- (14) Clancy, T. C.; Mattice, W. L. *J. Chem. Phys.* **2000**, *112*, 10049.
- (15) Dionne, P. J.; Ozisik, R.; Picu, R. C. *Macromolecules* **2005**, *38*, 9351.
- (16) Picu, R. C.; Ozmusul, M. *J. Chem. Phys.* **2003**, *118*, 11239.
- (17) Rouse, P. E. *J. Chem. Phys.* **1953**, *21*, 1272.
- (18) Smith, K.; Vladkov, M.; Barrat, J. L. *Macromolecules* **2005**, *38*, 571.
- (19) Zheng, X.; Sauer, B. B.; van Alsten, J. G.; Schwarz, S. A.; Rafailovich, M. H.; Sokolov, J.; Rubinstein, M. *Phys. Rev. Lett.* **1995**, *74*, 407.

MA0527754